

# MIDAS/GPP34, a nuclear gene product, regulates total mitochondrial mass in response to mitochondrial dysfunction

Naomi Nakashima-Kamimura<sup>1</sup>, Sadamitsu Asoh<sup>1</sup>, Yoshitomo Ishibashi<sup>1</sup>, Yuri Mukai<sup>1,\*</sup>, Yujiro Shidara<sup>1,2</sup>, Hideaki Oda<sup>2</sup>, Kae Munakata<sup>3</sup>, Yu-ichi Goto<sup>3</sup> and Shigeo Ohta<sup>1,‡</sup>

<sup>1</sup>Department of Biochemistry and Cell Biology, Institute of Development and Aging Sciences, Graduate School of Medicine, Nippon Medical School, 1-396 Kosugi-cho, Kawasaki, Kanagawa, 211-8533, Japan

<sup>2</sup>Department of Pathology, Tokyo Women's Medical University, School of Medicine, Shinjuku-ku, Tokyo, 162-8666, Japan

<sup>3</sup>Department of Mental Retardation and Birth Defect Research, National Institute of Neuroscience, NCNP, Kodaira, Tokyo, 187-8502, Japan

\*Present address: Computational Biology Research Center (CBRC), National Institute of Advanced Industrial Science and Technology (AIST), Koutou-ku, Tokyo, 135-0064, Japan

‡Author for correspondence (e-mail: ohta@nms.ac.jp)

Accepted 15 August 2005

Journal of Cell Science 118, 000-000 Published by The Company of Biologists 2005

doi:10.1242/jcs.02645

## Summary

To investigate the regulatory system in mitochondrial biogenesis involving crosstalk between the mitochondria and nucleus, we found a factor named MIDAS (mitochondrial DNA absence sensitive factor) whose expression was enhanced by the absence of mitochondrial DNA (mtDNA). In patients with mitochondrial diseases, MIDAS expression was increased only in dysfunctional muscle fibers. A majority of MIDAS localized to mitochondria with a small fraction in the Golgi apparatus in HeLa cells. To investigate the function of MIDAS, we stably transfected HeLa cells with an expression vector carrying MIDAS cDNA or siRNA. Cells expressing the MIDAS protein and the siRNA constitutively showed an increase and decrease in the total mass of mitochondria,

respectively, accompanying the regulation of a mitochondria-specific phospholipid, cardiolipin. In contrast, amounts of the mitochondrial DNA, RNA and proteins did not depend upon MIDAS. Thus, MIDAS is involved in the regulation of mitochondrial lipids, leading to increases of total mitochondrial mass in response to mitochondrial dysfunction.

Supplementary material available online at  
<http://jcs.biologists.org/cgi/content/full/118/22/5357/DC1>

Key words: Mitochondria, Mitochondrial mass, Cardiolipin, Mitochondrial DNA, Mitochondrial disease, Golgi apparatus

## Introduction

The mitochondrion is the center of energy metabolism in eukaryotes and has recently been recognized as a multifunctional organelle (Ohta, 2003). It is involved in the regulation of apoptosis as a reservoir of signals, regulators and executioners (Kroemer and Reed, 2000; Green and Kroemer, 2004). In addition, it functions as a source of reactive oxygen species, which are believed to cause many lifestyle-related diseases, neurodegenerative diseases, cancer and aging (Kowaltowski and Vercesi, 1999; Cortopassi and Wong, 1999; Melov, 2000). Thus, mitochondria are essential in many aspects of medicine as well as cell biology.

Depending on cell type, energy demands and physiological conditions, mitochondria vary in number, mass and morphology (Attardi and Schatz, 1988; Yaffe, 1999; Collins et al., 2002; Nisoli et al., 2003). The proliferation of cells usually accompanies an increase in mitochondria. However, an increase in number of mitochondria is not distinctly coordinated with the cell cycle. For example, muscle mitochondria increase in response to exercise, independently of cell division (Brunk, 1981; Moyes et al., 1997). Exposure to a low-temperature environment or cultivation in glucose-deprived medium induces a marked increase in mitochondrial

mass (Klaus et al., 1991; Weber et al., 2002). In addition, mitochondria increase in response to external stimuli with a wide range of substances including benzodiazepine, phorbol esters, calcium fluxes (Bereiter-Hahn and Voth, 1994; Vorobjev and Zorov, 1983; Muller-Hocker et al., 1986; Kawahara et al., 1991), thyroid hormones (Goglia et al., 1999) and nitric oxide (NO) (Nisoli et al., 2004). Mitochondrial numbers also increase in response to internal stimuli, such as the mitochondrial dysfunction caused by pathogenic mtDNA mutations (Schon, 2000; Wallace, 1999; Moraes et al., 1992). An increase in mitochondrial mass was observed in mitochondrial transcription factor A (*Tfam*) knockout mice, which have depleted mtDNA (Hansson et al., 2004).

As nuclear genes encode most mitochondrial proteins, including the enzymes and cofactors required for the transcription and replication of mtDNA, mitochondrial biogenesis depends on a distinct crosstalk between two physically separated genetic systems (Garesse and Vallejo, 2001). Recently, the pathway that links external physiological stimuli to the regulation of mitochondrial biogenesis and function has been studied. Several transcription/replication factors directly regulate mitochondrial genes and the

coordination of these factors into a programmed response to the environment was reported (Scarpulla, 2002).

However, the nature of mitochondrial biogenesis in response to internal stimuli is poorly understood. Mitochondrial stress results in enhanced expression of sarcoplasmic reticular ryanodine receptor-1 and some  $\text{Ca}^{2+}$ -responsive transcription factors (Biswas et al., 1999). Several tumor-specific markers are overexpressed in cells subjected to mitochondrial genetic as well as metabolic stress (Amuthan et al., 2001). Moreover, we have reported that expression of the apoptosis-mediator Fas is enhanced by dysfunctional mitochondria (Asoh et al., 1996). However, no one has reported on the mammalian factors, in response to a signal from mitochondria to the nucleus, which are involved in the stimulation of mitochondrial growth. Notably, the molecular mechanism regulating the biogenesis of mitochondrial lipids is poorly understood.

In this study, we identified factors whose expression was enhanced by depletion of mtDNA. One of them was found to increase total mitochondrial mass without a pathogenic swelling, when overexpressed. Thus, the factor is involved in the accumulation of mitochondria in response to mitochondrial dysfunction.

## Materials and Methods

### Cells and culture

EB8 and Ft2-11 were described previously (Hayashi et al., 1991; Hayashi et al., 1994). EB8 is a clone, derived from HeLa cells, completely lacking mtDNA, whereas Ft2-11 was constructed by transferring wild-type mtDNA into EB8 so that Ft-2-11 has the same nucleus as EB8. Stable transfectants expressing MIDAS constitutively were constructed from HeLa cells by transfection with *MIDAS* cDNA under the control of the CMV promoter or its empty vector (pCMV-SPORT; Life Technologies).

Stable transfectants expressing siRNA of *MIDAS* were constructed from HeLa cells by transfection with the pSilencer vector (Ambion) with inserts targeting *MIDAS* (5'-AAGCTTTTCCAAAAAGTGG-AATGTCTGAAGGCCATCTCTTGAATGGCCTTCAGACATTCC-ACGGGATCC-3') or a random sequence.

HeLa cells and stable transfectants were cultured in DMEM/F-12 (1:1) (Gibco-BRL) supplemented with 10% FBS and 1% penicillin/streptomycin (Gibco-BRL).

### Construction of Myc-tagged MIDAS

To insert the Myc tag at the N-terminus of MIDAS, an *EcoRI* site was generated at the 5' end of the *MIDAS* coding sequence by PCR and was cloned into the pCMV-SPORT vector. An oligonucleotide encoding MEQKLISEEDLNS (Myc tag sequence underlined) was inserted at the newly generated *EcoRI* site of *MIDAS*. To construct the Myc tag at the C-terminus of MIDAS, a *BamHI* site was generated at the 3' end of the coding sequence and an oligonucleotide encoding DPEQKLISEEDL was inserted.

### Differential display

Poly(A)<sup>+</sup> RNA was purified from Ft2-11 and EB8 and reverse transcribed. Resultant cDNAs were amplified using arbitrary primer sets, followed by 5% PAGE. The gel was stained with Vistra Green (Amersham Biosciences) and visualized with a Fluoro Imager (Molecular Dynamics) (Liang and Pardee, 1992).

### Antibodies

Anti-MIDAS polyclonal rabbit antiserum was raised against His-

tagged MIDAS expressed in *Escherichia coli*. Anti-MIDAS antibody was affinity purified by binding to the MIDAS protein isolated by SDS-PAGE, followed by transfer onto a PVDF membrane. Anti-Tom20 and anti-Tom40 were gifts from K. Mihara, Kyushu University, Japan. Other antibodies were purchased as follows: anti-actin (clone AC-40) and anti- $\beta$ -tubulin from Sigma; anti-p230 antibody and anti-Syntaxin6 from BD Biosciences; anti-Hsc70 antibody from Santa Cruz; anti-Hsp60 from MBL; anti-cytochrome c antibody and anti-Cox4 from Clontech; and anti-SDH70, anti-SDH30, anti-COX I and anti-COX II antibodies from Molecular Probes.

### Immunohistochemical staining of muscle sections

Biopsy samples were obtained from the biceps brachii muscle with informed consent and then frozen in isopentane and liquid nitrogen. Frozen sections 6  $\mu\text{m}$  thick were stained histochemically and immunologically. Activities of SDH and COX were visualized as described previously (Hasegawa et al., 1991; Dubowitz, 1985). The expression of MIDAS was detected with anti-MIDAS antibody. The polyclonal antibody against MIDAS was diluted 500-fold with 10% BSA in PBS and incubated with sections for 5 hours at 37°C and then MIDAS was detected with DAB using an indirect streptavidin-biotin immunohistochemical method, according to the manufacturer's protocol (Histofine, Nichirei, Co. Ltd., Tokyo, Japan). The MIDAS protein expressed was semi-quantified by the density of staining.

### Immunocytostaining of cultured cells

Cultured cells were fixed with 4% paraformaldehyde in PBS for 20 minutes at room temperature. After a wash with PBS, they were treated with 5% acetic acid in ethanol for 10 minutes at -20°C to permeabilize membranes, then incubated in a blocking buffer (3% BSA and 3% goat serum in PBS) and overnight at 4°C in the blocking buffer containing primary antibody. After another wash with PBS, the cells were incubated in the blocking buffer containing labeled secondary antibody and visualized with a confocal laser-scanning microscope (Fluoview FV300, Olympus, Tokyo, Japan). As an alternative, we used another method described (Bell et al., 2001). In brief, cells were fixed for 10 minutes with 4% paraformaldehyde and 4% sucrose without treatment for permeabilization and incubated with primary antibody, followed by secondary antibody.

### Subfractionation of HeLa cells

Cells were homogenized as described (Trounce et al., 1996). The homogenate was applied to a 7-35% (w/v) Nycodenz preformed continuous density gradient and centrifuged in a swinging-bucket rotor at 77,000  $g_{AV}$  for 4 hours. The fractions were collected from the top of the gradient. The MIDAS protein was semi-quantified by the density of total bands in western blots. The sub-organellar fractionation of mitochondria (fraction number 15) was performed as described (Kanamori et al., 2003).

### Electron microscopy

Cells were cultured on plastic dishes and fixed with 2% glutaraldehyde in PBS. Ultra-thin sections were stained with uranyl acetate and lead nitrate and examined with an H-7000 electron microscope (Hitachi, Tokyo, Japan).

### Flow cytometry

Living transfectants were stained with 20 nM MitoTracker Red CMXRos (Molecular Probes) or 100 nM MitoTracker Green (Molecular Probes) for 30 minutes at 37°C, treated with trypsin and subjected to a flow cytometric analysis with an Epics Elite ESP (Coulter).

### Three-dimensional imaging

Living cells were stained with 20 nM MitoTracker Red and 500 nM SYTO 16 (Molecular Probes) for 30 minutes at 37°C. The cells were scanned using 0.4  $\mu\text{m}$  sections with the confocal laser-scanning microscope. Three-dimensional (3D) views were reconstructed with Fluoview software (Olympus) and volumes of the nucleus and mitochondria were calculated by summing fluorescent areas from each section using the NIH Image program (developed at the US National Institutes of Health and available on <http://rsb.info.nih.gov/nih-image>).

### Separation of phospholipids

Total lipids were extracted from transfectants using methanol/chloroform as described (Folch et al., 1957). For the separation and detection of phospholipids, total lipids were injected into a HPLC system (model 616; Waters) fitted with a Wakosil 5Sil column (Wako, Tokyo, Japan). The mobile phase was a mixture of n-hexan, isopropanol, ethanol, acetic acid and 25 mM potassium phosphate buffer (pH 7.0) (146:282.5:50:0.3:31; v/v/v/v/v). The flow rate was 1 ml/minute. The elution of phospholipids was monitored at 205 nm with the UV detector (SPD-10A; Shimadzu). Retention times and quantities of phospholipids were determined using a phospholipid kit (Doosan Serdary Research Laboratory) as a standard.

## Results

### Cloning of genes that respond to a depletion of mtDNA

To identify nuclear genes that respond to a depletion of mtDNA, we screened for mRNA whose expression increased in cells lacking mtDNA using the differential mRNA display technique (Liang and Pardee, 1992) (Fig. 1A) by comparing mRNA populations in a HeLa derivative lacking mtDNA (EB8) (Hayashi et al., 1991) and control cybrid cells (Ft2-11) (Hayashi et al., 1994). Bands 1 and 2, which were stronger in EB8 than in Ft2-11 (Fig. 1A), were found to correspond to the apurinic/aprimidinic endonuclease I (APE1/HAP1) (Dempfle et al., 1991) and DNA ligase III genes (Wei et al., 1995), respectively. The products of these genes are localized in mitochondria and involved in mtDNA repair (Kang and Hamasaki, 2002).

DNA sequencing distinguished the gene corresponding to the third band in Fig. 1A from the genes which have been so far identified to be involved in mitochondrial biogenesis, gene expression and metabolism. The full-length cDNA was isolated from a human brain cDNA library (Gibco-BRL) to confirm the increase in its mRNA (Fig. 1B,C) and its product (Fig. 1D,E) by northern and western blotting, respectively. We named this gene *MIDAS* (mitochondrial DNA absence sensitive factor), because the gene product was expressed in response to mtDNA depletion. Interestingly, the nucleotide sequence was identical to *GPP34* (GenBank accession no. AJ296152) whose product has been identified as a Golgi protein of unknown function(s) (Bell et al., 2001). In addition, *MIDAS/GPP34* contains an isoform named *GPP34R* (GenBank accession no. AJ296153), which is highly homologous with *MIDAS/GPP34* (supplementary material Fig. S1). In fact, *GPP34R* was expressed in cells with the HeLa nucleus as detected by northern blotting (supplementary material Fig. S2A). Interestingly, *GPP34R* was also expressed more abundantly in EB8 than in Ft2-11 (supplementary material Fig. S2A). The relative amount of *GPP34R* mRNA was semi-quantified by the TaqMan probe method and found to be less than 2% of that in

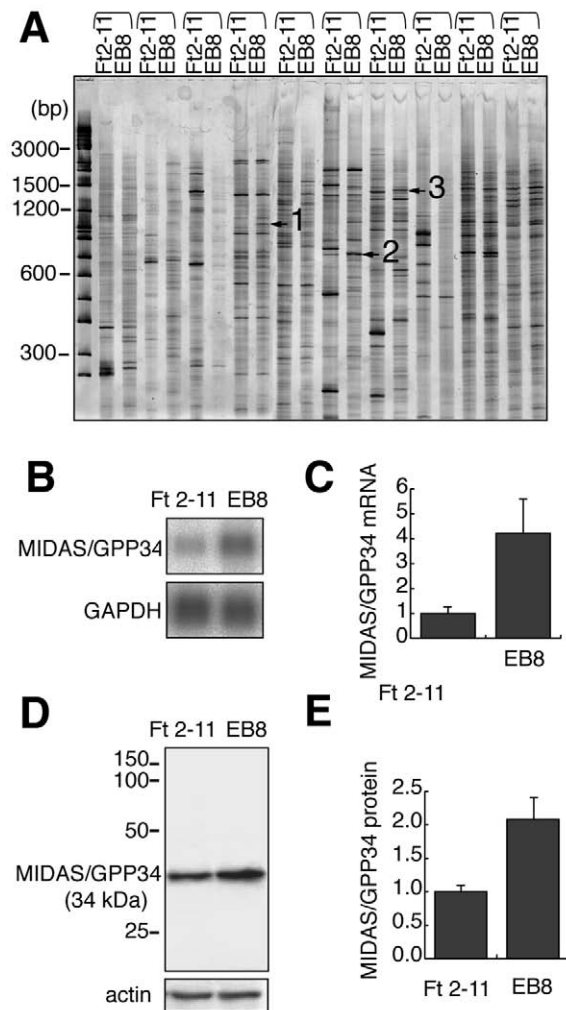


**Fig. 1.** Enhanced expression of *MIDAS/GPP34* in EB8 (mtDNA-free HeLa cells). (A) Comparison of mRNA obtained from Ft2-11 with that from EB8 by differential display. EB8 lacks mtDNA whereas Ft2-11 is derived from EB8 but has wild-type mitochondria. Ten sets of arbitrarily primed PCR products were subjected to 5% PAGE. Three bands indicated by arrows were cloned and sequenced. Bands 1, 2 and 3 corresponded to apurinic/aprimidinic endonuclease I, DNA ligase III and *MIDAS/GPP34*, respectively. (B) Northern blots of total RNA extracted from Ft2-11 and EB8 were hybridized with *GPP34*- and *GAPDH* (glyceraldehyde-3-phosphate dehydrogenase)-specific probes. (C) *GPP34* mRNA levels normalized to *GAPDH* levels based on the mean values  $\pm$  s.d. for three sets of northern blotting experiments (vertical bars). (D) Western blotting of Ft2-11 and EB8. Whole-cell lysates were separated by 12% SDS-PAGE and transferred onto a PVDF membrane. *MIDAS/GPP34* was immunostained with anti-*MIDAS* antibody. (E) The *MIDAS/GPP34* protein normalized against actin. Mean values of three sets of experiments are shown with s.d. (vertical bars).

*MIDAS/GPP34* (supplementary material Fig. S2B). Therefore, we focused on the function of *MIDAS/GPP34*.

### Specific expression of *MIDAS/GPP34* in muscle fibers with abnormal mitochondria

Mitochondria accumulate in response to their own dysfunction

in mitochondrial diseases (Schon, 2000; Wallace, 1999). We examined the expression of MIDAS/GPP34 in muscle fibers of patients with mitochondrial diseases. Large deletions and a point mutation in the tRNA<sup>Leu(UUR)</sup> gene of mtDNA are responsible for the subgroups of mitochondrial diseases, CPEO (chronic progressive external ophthalmoplegia) (Holt et al., 1988; Shoubridge et al., 1990) and MELAS (mitochondrial myopathy, encephalopathy, lactic acidosis and stroke-like episodes) (Goto et al., 1990; Kobayashi et al., 1990; Kobayashi et al., 1991), respectively. Accumulations of abnormal mitochondria are detected as ragged-red fibers and high succinate dehydrogenase (SDH) fibers, with mutant mtDNA dominating in a mosaic manner (Engel and Cunningham, 1963; Hasegawa et al., 1991; Lightowlers et al., 1997).

Muscle sections from a normal subject and patients with CPEO or MELAS were stained for activity of SDH and cytochrome c oxidase (COX) and with anti-MIDAS antibody. No MIDAS-positive fibers were detected in normal muscle, whereas MIDAS-positive fibers were detected in the muscle sections of affected patients (Fig. 2). The amount of MIDAS in the positive muscles increased approximately twofold compared to those in the negative muscles. It is noted that MIDAS was more abundant specifically in fibers with an SDH<sup>+</sup>/COX<sup>-</sup> phenotype (Fig. 2, asterisks). Thus, MIDAS is expressed in response to mitochondrial dysfunction in muscle with mitochondrial diseases.

#### Subcellular distribution of MIDAS/GPP34

GPP34 has been isolated as a Golgi peripheral membrane protein in a Golgi proteomics study (Bell et al., 2001). To verify the distribution of MIDAS in mitochondria, we immunostained HeLa cells with an affinity-purified polyclonal antibody against the MIDAS protein. Immunostaining of HeLa cells revealed that MIDAS mainly colocalized with MitoTracker Red (Fig. 3A). The mitochondrial localization was confirmed with another mitochondrial marker, Hsp60 (data not shown). With careful observation, we found MIDAS in an additional region, the perinuclear area, where MitoTracker Red was absent (Fig. 3A, merge; indicated by white arrowhead). This region corresponds to the Golgi apparatus, as judged by immunostaining with anti-p230 (the *trans*-Golgi membrane protein) (Erlach et al., 1996) antibody (Fig. 3B). These results suggest that a majority of MIDAS/GPP34 localizes to mitochondria, but some is distributed in the Golgi apparatus.

This finding disagrees with the previous study on GPP34 showing that GPP34 is located in the Golgi apparatus, but not in mitochondria (Bell et al., 2001). This discrepancy could be due to a different fixation method prior to staining. In general, for immunostaining of cultured cells, the permeabilization of intramembranes with an organic solvent or detergent is essential for antibodies to penetrate the membranes of organelles (Zeller, 1998). In fact, under the same conditions as the published experiment (no permeabilization pretreatment), MIDAS did not show colocalization with mitochondria (Fig. 3D), being detected only in the Golgi apparatus (Fig. 3E). Moreover, several marker proteins were immunostained to confirm that the permeabilization pretreatment with acetate in cold ethanol is essential for detecting the mitochondrial proteins located internally. Without permeabilization

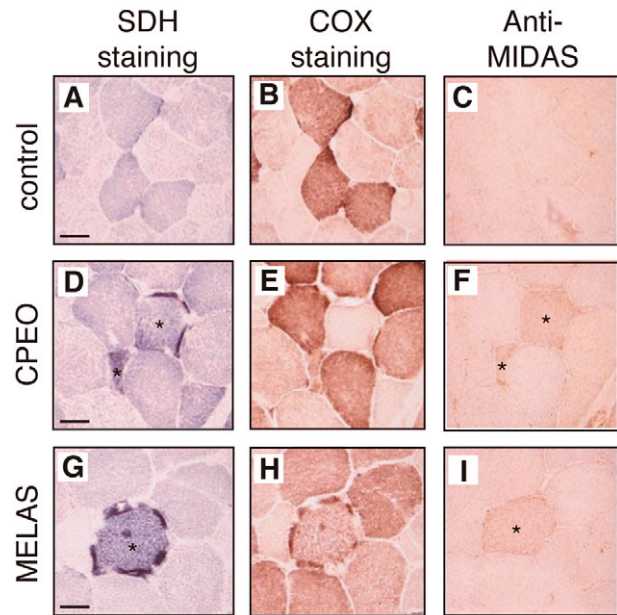


**Fig. 2.** Expression of MIDAS/GPP34 in SDH<sup>+</sup>/COX<sup>-</sup> muscle cells of patients with mitochondrial diseases. Biopsy samples were obtained from the biceps brachii muscle. Activities of SDH and COX were visualized histochemically and the expression of MIDAS/GPP34 was detected with anti-MIDAS antibody. (A–C) Control muscle without mitochondrial disorder. (D–F) Muscle from a patient with CPEO who has a common deletion in mtDNA. (G–I) Muscle from a patient with MELAS who has a point mutation at nucleotide number 3243 in the tRNA<sup>Leu(UUR)</sup> gene. Asterisks indicate SDH<sup>+</sup>/COX<sup>-</sup> cells of patients with increased MIDAS/GPP34 expression. Bars, 50  $\mu$ m.

pretreatment, cytosolic (Hsc70), mitochondrial outer membrane (Tom20) and *trans*-Golgi (p230) proteins were stained with each antibody (Fig. 3F), whereas the mitochondrial intermembrane space protein (cytochrome c) could not be detected (Fig. 3F). Alternatively, cytochrome c required an acetate/ethanol pretreatment for permeabilization as described in Materials and Methods to be detected (Fig. 3C). Moreover, a mitochondrial matrix protein (Hsp60) and an inner membrane protein (SDH70) were clearly stained only with the acetate/ethanol pretreatment (supplementary material Fig. S3). Therefore, the mitochondrial MIDAS/GPP34 protein is located inside mitochondria or embedded in the outer membrane. In addition, immunostaining with anti-KDEL, the signal peptide targeting the endoplasmic reticulum (ER) (Munro and Pelham, 1987), showed no localization of MIDAS/GPP34 to the ER (data not shown).

To further investigate the subcellular distribution of MIDAS, Myc-tagged constructs were generated. A gene corresponding to a Myc peptide was fused to the gene of the N-terminus (Myc-MIDAS) or C-terminus (MIDAS-Myc) of MIDAS. Fusion constructs were transfected into HeLa cells and the cells were allowed to express the protein for 16 hours. The transfected cells were immunostained with anti-Myc antibody. Myc-MIDAS was localized to the perinuclear area and colocalized with the p230 *trans*-Golgi (Fig. 3G). On the other hand, MIDAS-Myc was distributed in both mitochondria and Golgi as stained with anti-MIDAS antibody (Fig. 3H). This

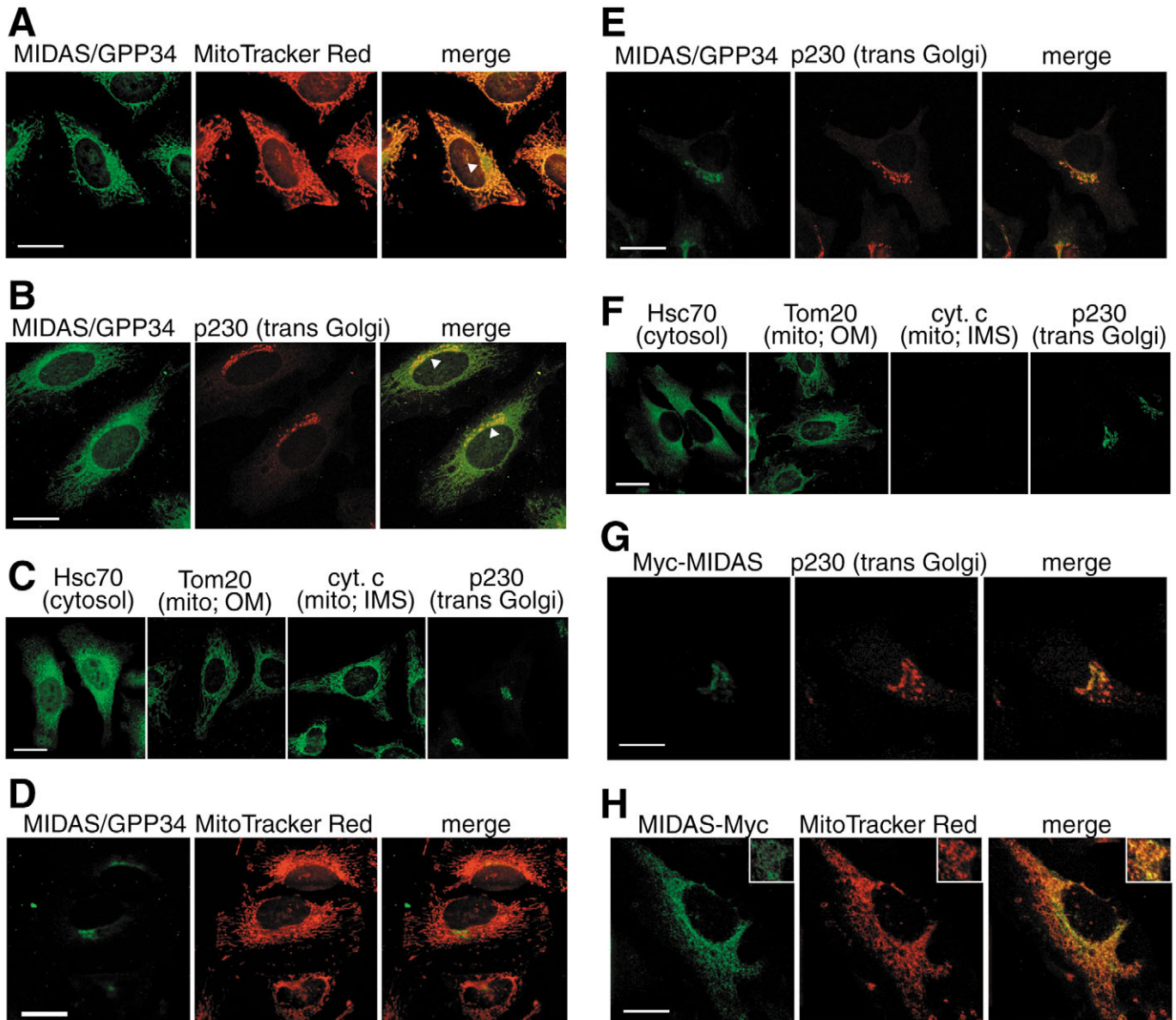


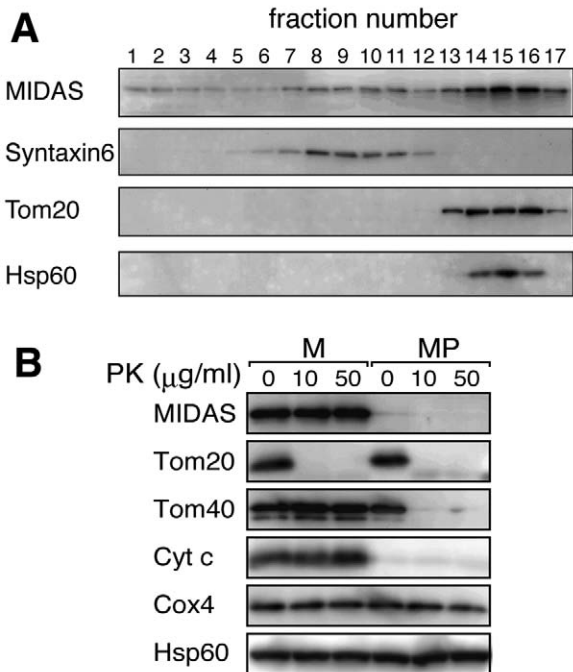
**Fig. 3.** Localization of MIDAS/GPP34 in mitochondria and the Golgi apparatus. (A-C) HeLa cells in culture were fixed, permeabilized with 5% acetic acid in ethanol and then immunostained with various antibodies. (A) MitoTracker Red (100 nM) was added as a mitochondrial indicator prior to fixation. MIDAS/GPP34 was detected with anti-MIDAS antibody. Arrowhead indicates where MIDAS/GPP34 is more abundant than mitochondria in a perinuclear area. (B) MIDAS/GPP34 and p230 (*trans*-Golgi) were double-stained immunochemically using different secondary antibodies. Arrowheads indicate where the perinuclear area was co-stained with both antibodies. (C) Hsc70 (cytosol), Tom20 (outer membrane of mitochondria), cytochrome c (cyt. c) (intermembrane space of mitochondria) and p230 (*trans*-Golgi) were detected with their respective antibodies. (D-F) HeLa cells in culture were fixed with 4% paraformaldehyde and 4% sucrose without treatment for permeabilization and immunostained with the same procedure as in (A-C). (G,H) Localization of Myc-tagged MIDAS. A Myc tag was fused to the N-terminus (G) or C-terminus (H) of MIDAS. Fusion constructs were transfected into HeLa cells and cells were allowed to express protein for 16 hours. Cells were stained with anti-Myc, anti-p230 antibodies or MitoTracker Red with the same procedure as in (A-C). Bars, 20  $\mu$ m.

finding suggests that MIDAS potentially localizes to both mitochondria and the Golgi apparatus.

To demonstrate the subcellular distribution of MIDAS, organelles were sub-fractionated with a Nycodenz gradient. HeLa cells were homogenized, the homogenate was fractionated with a 7-35% density gradient and the distribution of MIDAS was examined by western blotting (Fig. 4A). The majority of MIDAS was detected in the mitochondrial fractions

(with Tom20 and Hsp60) and small portions were fractionated with the Golgi (with a Golgi marker, Syntaxin6) and cytosol. Relative amounts of MIDAS distributed in the fractions for mitochondria (fractions 13-17), Golgi (fractions 6-12) and cytosol (fractions 1-5) were 0.75, 0.19 and 0.06, respectively, as judged by the densities of total bands.

To determine the sub-mitochondrial distribution of MIDAS, the mitochondria purified from HeLa cells were treated with



proteinase K. Both Tom40 and Tom20 are embedded in the outer membrane, whereas Tom20 is exposed to the outside of mitochondria (Pfanner and Geissler, 2001). Tom20 was easily digested with 10  $\mu\text{g/ml}$  proteinase K, whereas Tom40 and MIDAS were resistant (Fig. 4B, M). On the other hand, when mitochondria were converted to mitoplasts, MIDAS disappeared (Fig. 4B, MP) even without proteinase K, as cytochrome *c* disappeared. From these results, it was concluded that the majority of MIDAS protein is located in the

**Fig. 4.** Localization of MIDAS/GPP34 in the mitochondrial intermembrane space. (A) Fractionation of organelles of HeLa cells in 7–35% (w/v) preformed density gradients. The distribution of MIDAS was detected by western blotting. Syntaxin6 was used for a Golgi marker. Tom20 and Hsp60 were used for mitochondrial markers. (B) Mitoplasts were obtained from the mitochondrial fraction (fraction 15 in A) by osmotic disruption of the outer membrane. The mitochondria (M; lanes 1–3) and the mitoplasts (MP; lanes 4–6) were treated with proteinase K (PK; 10  $\mu\text{g/ml}$  or 50  $\mu\text{g/ml}$ ). Mitochondrial sub-fractions were monitored by western blotting with antibodies directed against Tom20 (an outer membrane protein; most of which is exposed outside mitochondria), Tom40 (an outer membrane protein), cytochrome *c* (cyt *c*) (an intermembrane space protein), Cox4 (an inner membrane protein) and Hsp60 (a matrix space protein).

intermembrane space of mitochondria, with a small fraction present in the Golgi apparatus.

#### Mitochondrial accumulation without swelling by MIDAS

To determine the function of MIDAS in mitochondria, HeLa cells were transfected with *MIDAS* cDNA under the control of the CMV promoter. We could isolate transfectants constitutively expressing MIDAS at low levels (1.5- to 2-fold increase) (Fig. 5A, upper left panel, CMV-MIDAS3 and CMV-MIDAS9). Cells transiently transfected with a higher level of MIDAS could undergo cell division once or twice but did not survive for a week (data not shown), suggesting that overproduction of MIDAS prevents cell growth. To downregulate MIDAS, we then constructed HeLa transfectants expressing siRNA (small interfering RNA) of *MIDAS* to inhibit the endogenous *MIDAS* expression (Fig. 5A, upper right panel).

These transfectants were stained with MitoTracker Red to visualize mitochondria, in a short period to monitor the membrane potential of mitochondria. Even low levels of additional MIDAS expression caused a change in the distribution of mitochondria. The mitochondria in a *MIDAS* transfectant CMV-MIDAS3 were concentrated around the nucleus (Fig. 5B, second panel), whereas those in the control transfectants remained dispersed (Fig. 5B, first panel).

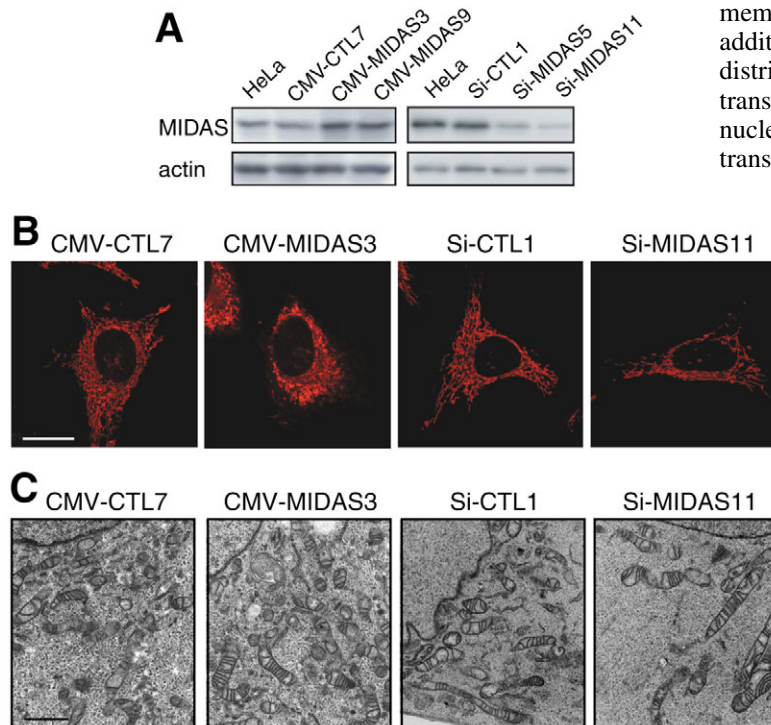


**Fig. 5.** The increased or decreased mass of intact mitochondria related to MIDAS concentration. (A) CMV-CTL7 and Si-CTL1 are stable control transfectants derived from HeLa cells. Although CMV-MIDAS3 and CMV-MIDAS9 are stable *MIDAS* transfectants under the control of the CMV promoter. Si-MIDAS5 and Si-MIDAS11 were transfectants expressing siRNA of *MIDAS* constitutively. Total cell lysate was extracted from each transfectant cell line and subjected to western blotting with anti-MIDAS and anti-actin antibodies. (B) Control (CMV-CTL7 and Si-CTL1), *MIDAS* transfectants (CMV-MIDAS3) and siRNA *MIDAS* transfectants (Si-MIDAS11) were stained with MitoTracker Red and visualized by confocal scanning laser microscopy. (C) Electron micrographs ( $\times 8000$ ) of mitochondria in the transfectants. Bar, 20  $\mu\text{m}$  (B); 1  $\mu\text{m}$  (C).

Moreover, mitochondria in the MIDAS-expressing transfectants were stained more strongly than those in the control cells. Another transfectant clone CMV-MIDAS9 showed the same results (data not shown).

The mitochondria in a siRNA *MIDAS* transfectant, Si-MIDAS11, were dispersed similarly to those in the control transfectant (Si-CTL1) but were less intensely stained (Fig. 5B, third and fourth panels). Another siRNA *MIDAS* transfectant, clone Si-MIDAS5, showed the same results (data not shown).

Electron microscopy showed that mitochondria in the *MIDAS* transfectant were somewhat larger with no marked change in morphology and were neither pathologically swollen nor had lost the cristae structure (Fig. 5C, second panel). In addition, the *MIDAS* transfectants increased the number of mitochondria, whereas the siRNA-transfectants decreased the number of mitochondria (Fig. 5C, fourth panel). These photographs suggest that the number of mitochondria around the nucleus was increased by MIDAS.

#### Increase in total mitochondrial mass by MIDAS

To quantify the accumulation of mitochondria suggested above, cells were stained with two mitochondria-specific dyes, MitoTracker Red and MitoTracker Green and subjected to flow cytometric analysis (Fig. 6A-C). There was no significant difference in forward scatter among any of the cells examined (FS in Fig. 6C), indicating that MIDAS does not have any influence on cell size, regardless of the up- or downregulation of its expression. MitoTracker Green, but not MitoTracker Red, binds to mitochondria in a membrane-potential-independent manner and fluoresces only in the lipid environment of mitochondria. Fluorescent intensity in green (MitoTracker Green) was measured to estimate overall mitochondrial mass, whereas fluorescent intensity in red (MitoTracker Red) was measured to assess the content of energized mitochondria. The intensities in green and red significantly increased in MIDAS-expressing transfectants (CMV-MIDAS) (Fig. 6A,C). On the other hand, the green and red intensities decreased in the MIDAS downregulated transfectants (Si-MIDAS) (Fig. 6B,C). Quantitative analysis showed that the fluorescent intensities increased 1.5- to 2-fold in the MIDAS-expressing transfectants and decreased to 60-70% in the downregulated transfectants, compared to the control cells, respectively (Fig. 6C). The ratio of the intensity in red to the intensity in green was the same in all the cells examined, indicating that MIDAS does not exert any influence on the membrane potential. To confirm the increase in mitochondria, we stained transfectants with an additional fluorescent dye, TMRM (tetra-methyl-rhodamine methyl ester) specific to mitochondria and obtained a consistent result (supplementary material Fig. S4).

The increase in the fluorescence of MitoTracker Green strongly suggests a substantial increase in total mitochondrial mass caused by MIDAS. Therefore, we estimated total mitochondrial volume by three-dimensional reconstitution of

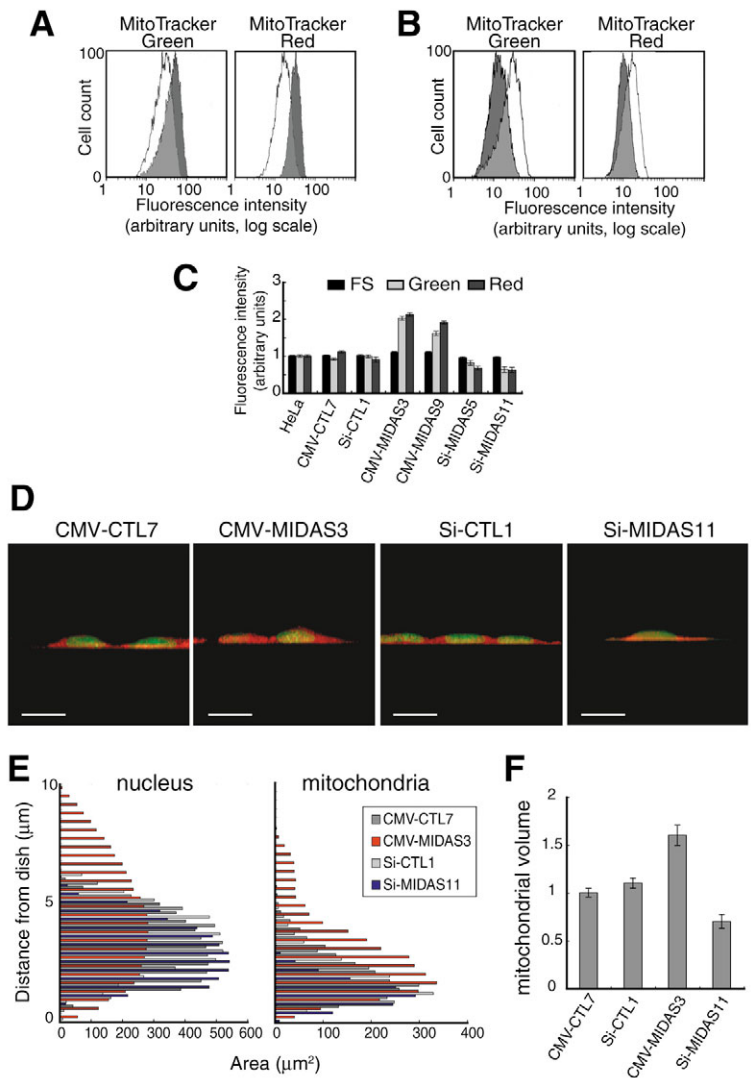


**Fig. 6.** Changes in mitochondrial mass with MIDAS. (A) Flow cytometric profiles of the fluorescence of dyes specific to mitochondria in CMV-CTL7 (white) and CMV-MIDAS3 (gray). Living transfectants were stained with MitoTracker Green (left) or MitoTracker Red (right) and analyzed with a flow cytometer. (B) Flow cytometric analysis performed with Si-CTL1 (white) and Si-MIDAS11 (gray) cells as described in A. (C) Fluorescence intensity (MitoTracker Green and MitoTracker Red) as well as forward scatter (FS) of HeLa cells and transfectants as quantified by flow cytometry. Values are the mean  $\pm$  s.d. (D) The mitochondria and nucleus in control transfectants (CMV-CTL7 and Si-CTL1), *MIDAS* transfectants (CMV-MIDAS3) and siRNA *MIDAS* transfectants (Si-MIDAS11) were stained with MitoTracker Red and SYTO 16 (green), respectively and scanned by confocal laser microscopy in each 0.4  $\mu$ m section. Then the side view of a three-dimensional image was reconstructed with Fluoview software. (E) Areas of the nucleus and mitochondria were measured for each section. (F) The total mass of mitochondria in the transfectants was calculated based on the values in E and normalized to that of nucleus. Data represent the mean  $\pm$  s.d. of three sets of experiments. Bars, 20  $\mu$ m.

cells. Cells were stained with MitoTracker Red (red) for mitochondria and SYTO 16 (green) for the nucleus, respectively. The cells were scanned from bottom to top at intervals of 0.4  $\mu$ m and each image was analyzed to measure the areas stained with MitoTracker Red and SYTO 16,

separately (Fig. 6E). Interestingly, the side view of the reconstituted three-dimensional image showed that mitochondria in the transfectants expressing MIDAS accumulated at the periphery of the nucleus (Fig. 6D, second panel), whereas in the downregulated transfectants, mitochondria appeared to be decreased in number (Fig. 6D, fourth panel). It is noted that there was no difference in nuclear volume between cells, although their three-dimensional shapes were different. On average, mitochondria occupied 22%, 35% and 15% of the total cytoplasm in controls, MIDAS-expressing transfectants and siRNA transfectants, respectively. The total volume of mitochondria was increased 1.6-fold by the MIDAS expression and decreased 0.75-fold by the downregulation of MIDAS, when normalized to that of the nucleus (Fig. 6F). Thus, the total mitochondrial mass varied more than 2.3-fold with the up- and downregulation of MIDAS. These results clearly indicate that MIDAS regulates total mitochondrial mass.

### Regulation of cardiolipin by MIDAS

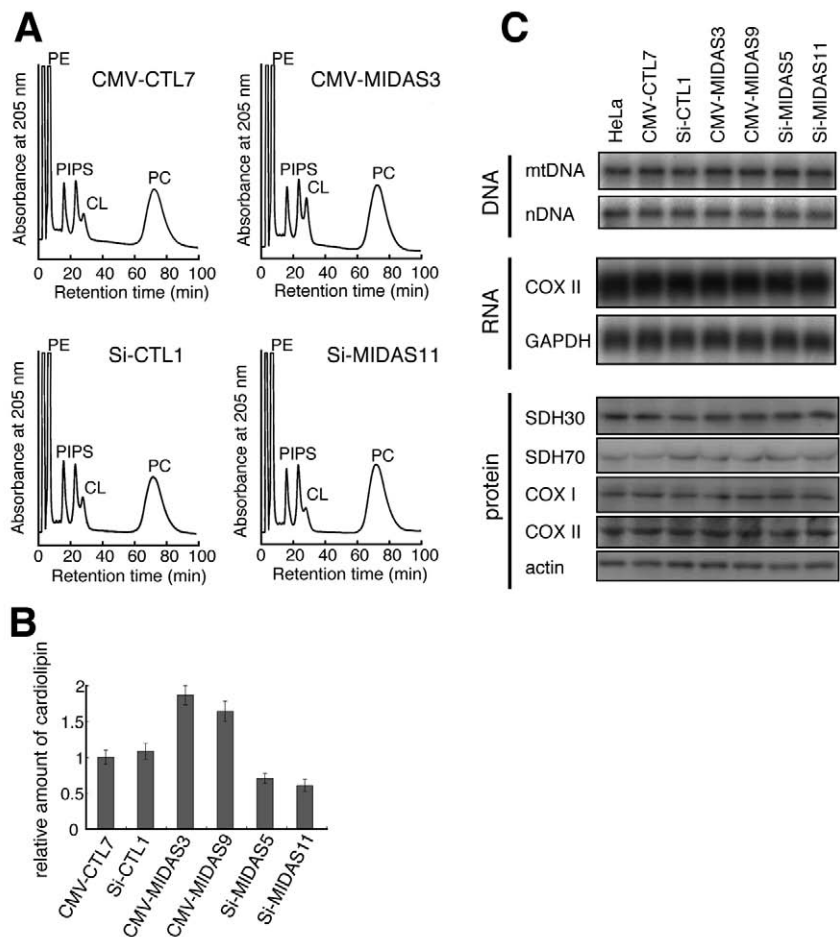
Flow cytometric analysis using MitoTracker Green showed that mitochondrial lipids varied in a MIDAS-dependent manner. Furthermore, the analysis using the fluorescent dye NAO (nonyl acridine orange), which detects cardiolipin, a mitochondria-specific phospholipid, revealed that the amount of cardiolipin varied according to amount of MIDAS

(supplementary material Fig. S5). To obtain direct evidence for an increase in mitochondrial lipids caused by MIDAS, we measured levels of cardiolipin by HPLC. Total lipids were extracted from each transfectant and separated by HPLC as described in the Materials and Methods (Fig. 7A). The peak of cardiolipin (CL) was found to increase in MIDAS-expressing transfectants, compared with control transfectants. In clear contrast, the CL peak decreased in the MIDAS downregulated transfectants. The relative amount of each phospholipid was quantified based on the HPLC peak (Fig. 7B). The results showed that the amount of cardiolipin was increased 1.75-fold in the MIDAS-expressing transfectant and decreased 0.65-fold in the downregulated transfectant, when normalized to that of phosphatidylcholine. Thus, the amount of cardiolipin varied more than 2.6-fold with the up- and downregulation of MIDAS.

### Mitochondrial DNA, RNA and proteins were not affected by MIDAS

To understand the mitochondrial increase induced by MIDAS, we examined other mitochondrial components, mitochondrial DNA, RNA and proteins (Fig. 7C). The amount of mtDNA was analyzed by Southern blotting and no significant change was observed. Northern blotting also revealed no change in the stationary amounts of COX II mRNA transcribed from mtDNA. Immunoblots revealed no increase in mitochondrion-

**Fig. 7.** Effects of MIDAS on amounts of cardiolipin (a mitochondria-specific lipid), mitochondrial DNA, RNA and proteins. (A) Total lipids were extracted from control transfectants (CMV-CTL7 and Si-CTL1), MIDAS transfectants (CMV-MIDAS3) and siRNA MIDAS transfectants (Si-MIDAS11) and fractionated by HPLC as described in the Materials and Methods. The elution of phospholipids was monitored at 205 nm. CL, cardiolipin; PC, phosphatidylcholine; PE, phosphatidylethanolamine; PI, phosphatidylinositol; PS, phosphatidylserine. (B) The amount of cardiolipin in the transfectants was quantified based on the values in A and normalized to that of phosphatidylcholine. Mean values for three sets of experiments are shown with the s.d. (C) The amount of DNA in HeLa cells and transfectants was analyzed by Southern blotting. To detect mtDNA we used the COX II region in mtDNA as a probe. The nDNA (nuclear DNA) was a loading control and the 18S ribosomal DNA region was used as a probe. The expression of mtDNA and nDNA was analyzed by northern blotting. Blots of total RNA extracted from HeLa and transfectants were hybridized with *COX II*- and *GAPDH*-specific probes. Proteins were analyzed by western blotting. SDH30 and SDH70 are the nucleus-encoded 30 kDa and 70 kDa subunit of SDH, respectively. COX I and COX II are the mitochondrial DNA-encoded subunits.



encoded proteins, COX I and COX II and nucleus-encoded mitochondrial proteins, the 30 kDa and 70 kDa subunits of SDH.

## Discussion

In this study, we found three nuclear genes that respond to the depletion of mtDNA. Although mtDNA was completely depleted after a long exposure of HeLa cells to ethidium bromide, its nuclear genes may be affected at a high frequency. Thus, we used a cybrid clone, Ft2-11, that had been obtained by the intercellular transfer of wild-type mitochondria into EB8 cells as a control instead of parental HeLa cells. This procedure, cell fusion between enucleated cells (mitochondrion donor) and EB8 cells, would cause no damage to the nuclear genes.

On comparing the mRNA isolated from EB8 cells with that of control cells by differential display, we found three genes whose expression was higher in EB8 cells. Two of them were the apurinic/aprimidinic endonuclease I (APE1/HAP1) (Demple et al., 1991) and DNA ligase III genes (Wei et al., 1995). These gene products are located in mitochondria as well as the nucleus and are involved in DNA repair. Thus, it is reasonable to assume that the mitochondrial repair system responds to the depletion of mtDNA.

The third gene product, named MIDAS here, was identical to a Golgi protein, GPP34. The nucleotide sequence of *MIDAS/GPP34* is conserved from yeast to human (Bell et al., 2001; Wu et al., 2000). Its yeast *Saccharomyces cerevisiae* homolog (YDR372c) has been deleted revealing that the gene is not essential for viability (Winzler et al., 1999; Bidlingmaier and Snyder, 2002). Although a mutation in the YDR372c gene revealed a phenotype with an abnormal budding (Bidlingmaier and Snyder, 2002) and aberrant in protein-vacuolar targeting (Bonangelino et al., 2002), the molecular function of the gene product remains unknown. Genetic analysis showed that there are genetic interactions between YDR372c and intracellular protein-transport factors (RIC1 and YPT6) (Tong et al., 2004). As MIDAS has a leucine-zipper motif (supplementary material Fig. S1), it may interact with a protein involved in intracellular protein transport through this motif.

In most mitochondrial diseases, mutant mtDNA coexists with wild-type mtDNA at various ratios in a heteroplasmic manner and exhibits a cognate pathological phenotype in a threshold-dependent manner. COX-deficient cells have abundant mutant mtDNA, whereas COX-positive cells have a small amount of mutant mtDNA. MIDAS was shown to be more abundant in muscle cells with no COX activity in patients with mitochondrial diseases. This finding indicates that the enhanced expression of MIDAS occurs not only in HeLa cells lacking mtDNA, but also in muscle cells with pathogenic mutant mtDNAs, regardless of point mutations or deletions of mtDNA. MIDAS has putative ATF-1 binding sites and the upregulated expression by EWS/ATF-1 chimeric transcription factor was revealed (Jishage et al., 2003). When mitochondrial dysfunction occurs, the expression of MIDAS may be activated by CREB/ATF-1 family transcription factors.

A previous report (Bell et al., 2001) indicated that GPP34 colocalizes only with Golgi, but not mitochondria. When we used the method they described (Bell et al., 2001) with

permeabilization pretreatment after fixation, anti-MIDAS antibody stained only the Golgi apparatus (Fig. 3D,E). On the other hand, immunostaining clearly showed that MIDAS colocalized with both mitochondria and the Golgi apparatus when the cells were subjected to the acetate/ethanol pretreatment to permeabilize the mitochondrial membranes. An outer membrane protein (Tom 20) did not require the permeabilization procedure for staining, but the acetate/ethanol procedure was essential for the proteins located inside mitochondria such as cytochrome c, Hsp60 and SDH70 (Fig. 3C and supplementary material Fig. S3). Thus, the discrepancy is fully explained by the difference in the permeabilization method used (Fig. 3). The present result is consistent with the result of a sub-organellar fractionation experiment that showed that MIDAS is present in the intermembrane space. Thus, it is concluded that the antibody against MIDAS/GPP34 cannot access the mitochondrial MIDAS without the permeabilization pretreatment. As MIDAS lacks typical sequences that could target mitochondria or the Golgi apparatus, it is unknown how it is directed to the respective organelle.

As MIDAS/GPP34 has an isoform, named GPP34R, one may target mitochondria and the other may target the Golgi apparatus. However, this is unlikely because GPP34R was expressed at a level less than 2% of that of MIDAS in HeLa cells. This small amount cannot account for the relative amount of the protein located in the Golgi apparatus. In addition, we performed a crucial experiment. As the fusion protein comprising Myc-tag and the N-terminus of MIDAS targets only Golgi, the N-terminal region may be responsible for targeting mitochondria. In contrast, an alternative fusion protein with Myc-tag at the C-terminus of MIDAS targets mitochondria. This experiment suggests that the single molecule has the potential to localize to two distinct organelles. Further experiments will reveal which location of MIDAS contributes to its distribution.

Mitochondria gathered around the nucleus in MIDAS-expressing transfectants. As mitochondria often gather around the nucleus in sick cells regardless of internal or external conditions, it may be that toxicity of MIDAS forces mitochondria to concentrate around the nucleus by affecting the cytoskeletal structure. However, no abnormal cytoskeletal structure was found in MIDAS-expressing transfectants (supplementary material Fig. S6). Thus, the mitochondrial accumulation was not due to abnormality of the cytoskeleton. The mitochondrial biogenesis occurs near the nucleus and fresh mitochondria are transported to peripheral areas (Yaffe, 1999). Thus, newly synthesized mitochondria seem to be concentrated around the nucleus and then the excess mitochondria may push up the nucleus as seen in Fig. 5B and Fig. 6D, second panel.

A transcriptional coactivator PGC-1 enhances the expression of many mitochondrial proteins by activating several transcription factors, such as NRF-1, NRF-2, Sp1, YY1, CREB and MEF-2/E-box (Scarpulla, 2002). Recognition sites for NRF-1, NRF-2 and Sp1 are common to most nuclear genes encoding components involved in mitochondrial respiration, transcription and replication (Scarpulla, 2002). However, it is unknown how PGC-1 contributes to the increase in mitochondrial lipids. In addition, there has been no report that PGC-1 is expressed in response to mitochondrial dysfunction or damage. MIDAS seems to accumulate mitochondria by an

alternative pathway from PGC-1 because MIDAS did not enhance mitochondrial transcription (Fig. 7C).

As mitochondria dynamically repeat fusion and fission, it is difficult to clarify their number (Griparic and van der Bliek, 2001; Westermann, 2002). In this study, we thus paid attention to the total mass of mitochondria. Three-dimensional imaging revealed a change in the total mass of mitochondria. The increase was 1.6-fold, which agrees with the increase in strength of the fluorescence of MitoTracker Red and MitoTracker Green in MIDAS-expressing transfectants. This increase is not so small because mitochondria occupy more than 20% of the total volume of the cytoplasm in HeLa cells. When the downregulation and upregulation of MIDAS were compared, the total mass was found to vary more than 2.3-fold from 15% to 35% of the total cytoplasm of HeLa cells. Thus, MIDAS dramatically regulates the total mitochondrial mass.

Mitochondria are often swollen pathogenically or by an increase of cytosolic  $\text{Ca}^{2+}$ . It may be that the mitochondria are simply swollen owing to the expression of MIDAS. However, this is unlikely for the following reasons. First, the ratio of the intensity in red to the intensity in green was the same in all the cells examined, indicating that MIDAS does not exert any influence on membrane potential (Fig. 6C). Although MIDAS-expressing cells have lower concentrations of mitochondrial protein per volume than controls (Fig. 7C), the levels seem high enough for membrane potential. Second, the downregulation of MIDAS conversely decreased the total mass of mitochondria. Third, mitochondria appear intact morphologically, being independent of the up- or downregulation of MIDAS (Fig. 5C). Finally, it is crucial that the amount of cardiolipin varied depending upon the amount of MIDAS and that the extent of the change was well correlated with the total mass of mitochondria that was revealed by three-dimensional imaging. Cardiolipin is a mitochondrion-specific lipid but accounts for only 20% of mitochondrial lipids. This suggests that not only the amount of cardiolipin but also the total amount of mitochondrial lipids is changed by MIDAS. Taken together, it is concluded that total mitochondrial mass is regulated by MIDAS through the biogenesis of mitochondrial lipids.

The molecular mechanism by which the MIDAS protein increases production of cardiolipin is unknown. A detailed analysis of the *MIDAS* gene and the function of MIDAS should provide insight into the molecular mechanism by which mitochondrial dysfunction is sensed to increase mitochondria. The fact that MIDAS is colocalized with both mitochondria and the Golgi apparatus may be a key to answering the question of how lipids contribute to mitochondrial accumulation.

We thank K. Mihara of Kyushu University for the gift of anti-Tom20 and anti-Tom40 antibodies, I. Ohsawa and T. Kanamori for helpful advice and K. Yamagata for technical assistance.

## References

- Amuthan, G., Biswas, G., Zhang, S. Y., Klein-Szanto, A., Vijayasarathy, C. and Avadhani, N. G. (2001). Mitochondria-to-nucleus stress signaling induces phenotypic changes, tumor progression and cell invasion. *EMBO J.* **20**, 1910-1920.
- Asoh, S., Mori, T., Hayashi, J. and Ohta, S. (1996). Expression of the apoptosis-mediator Fas is enhanced by dysfunctional mitochondria. *J. Biochem. (Tokyo)* **120**, 600-607.
- Attardi, G. and Schatz, G. (1988). Biogenesis of mitochondria. *Annu. Rev. Cell Biol.* **4**, 289-333.
- Bell, A. W., Ward, M. A., Blackstock, W. P., Freeman, H. N., Choudhary, J. S., Lewis, A. P., Chotai, D., Fazel, A., Gushue, J. N., Paiement, J. et al. (2001). Proteomics characterization of abundant Golgi membrane proteins. *J. Biol. Chem.* **276**, 5152-5165.
- Bereiter-Hahn, J. and Voth, M. (1994). Dynamics of mitochondria in living cells: shape changes, dislocations, fusion and fission of mitochondria. *Microsc. Res. Tech.* **27**, 198-219.
- Bidlingmaier, S. and Snyder, M. (2002). Large-scale identification of genes important for apical growth in *Saccharomyces cerevisiae* by directed allele replacement technology (DART) screening. *Funct. Integr. Genomics* **1**, 345-356.
- Biswas, G., Adebajo, O. A., Freedman, B. D., Anandatheerthavarada, H. K., Vijayasarathy, C., Zaidi, M., Kotlikoff, M. and Avadhani, N. G. (1999). Retrograde  $\text{Ca}^{2+}$  signaling in C2C12 skeletal myocytes in response to mitochondrial genetic and metabolic stress: a novel mode of inter-organelle crosstalk. *EMBO J.* **18**, 522-533.
- Bonangelino, C. J., Chavez, E. M. and Bonifacino, J. S. (2002). Genomic screen for vacuolar protein sorting genes in *Saccharomyces cerevisiae*. *Mol. Biol. Cell* **13**, 2486-2501.
- Brunk, C. F. (1981). Mitochondrial proliferation during myogenesis. *Exp. Cell Res.* **136**, 305-309.
- Collins, T. J., Berridge, M. J., Lipp, P. and Bootman, M. D. (2002). Mitochondria are morphologically and functionally heterogeneous within cells. *EMBO J.* **21**, 1616-1627.
- Cortopassi, G. A. and Wong, A. (1999). Mitochondria in organismal aging and degeneration. *Biochim. Biophys. Acta* **1410**, 183-193.
- Demple, B., Herman, T. and Chen, D. S. (1991). Cloning and expression of APE, the cDNA encoding the major human apurinic endonuclease: definition of a family of DNA repair enzymes. *Proc. Natl. Acad. Sci. USA* **88**, 11450-11454.
- Dubowitz, V. (1985). Histological and histochemical stains and reactions. In *Muscle Biopsy: a practical approach*, 2nd edn, (ed. V. Dubowitz), pp. 19-40. London: Balliere Tindall.
- Engel, W. K. and Cunningham, G. G. (1963). Rapid examination of muscle tissue. An improved trichrome method for fresh-frozen biopsy sections. *Neurology* **13**, 919-926.
- Erlich, R., Gleeson, P. A., Campbell, P., Dietzsch, E. and Toh, B. H. (1996). Molecular characterization of *trans*-Golgi p230. A human peripheral membrane protein encoded by a gene on chromosome 6p12-22 contains extensive coiled-coil alpha-helical domains and a granin motif. *J. Biol. Chem.* **271**, 8328-8337.
- Folch, J., Lees, M. and Sloane Stanley, G. H. (1957). A simple method for the isolation and purification of total lipides from animal tissues. *J. Biol. Chem.* **226**, 497-509.
- Garesse, R. and Vallejo, C. G. (2001). Animal mitochondrial biogenesis and function: a regulatory cross-talk between two genomes. *Gene* **263**, 1-16.
- Goglia, F., Moreno, M. and Lanni, A. (1999). Action of thyroid hormones at the cellular level: the mitochondrial target. *FEBS Lett.* **452**, 115-120.
- Goto, Y., Nonaka, I. and Horai, S. (1990). A mutation in the tRNA<sup>Leu(UUR)</sup> gene associated with the MELAS subgroup of mitochondrial encephalomyopathies. *Nature* **348**, 651-653.
- Green, D. R. and Kroemer, G. (2004). The pathophysiology of mitochondrial cell death. *Science* **305**, 626-629.
- Griparic, L. and van der Bliek, A. M. (2001). The many shapes of mitochondrial membranes. *Traffic* **2**, 235-244.
- Hansson, A., Hance, N., Dufour, E., Rantanen, A., Hultenby, K., Clayton, D. A., Wibom, R. and Larsson, N. G. (2004). A switch in metabolism precedes increased mitochondrial biogenesis in respiratory chain-deficient mouse hearts. *Proc. Natl. Acad. Sci. USA* **101**, 3136-3141.
- Hasegawa, H., Matsuoka, T., Goto, Y. and Nonaka, I. (1991). Strongly succinate dehydrogenase-reactive blood vessels in muscles from patients with mitochondrial myopathy, encephalopathy, lactic acidosis and stroke-like episodes. *Ann. Neurol.* **29**, 601-605.
- Hayashi, J., Ohta, S., Kikuchi, A., Takemitsu, M., Goto, Y. and Nonaka, I. (1991). Introduction of disease-related mitochondrial DNA deletions into HeLa cells lacking mitochondrial DNA results in mitochondrial dysfunction. *Proc. Natl. Acad. Sci. USA* **88**, 10614-10618.
- Hayashi, J., Ohta, S., Kagawa, Y., Kondo, H., Kaneda, H., Yonekawa, H., Takai, D. and Miyabayashi, S. (1994). Nuclear but not mitochondrial genome involvement in human age-related mitochondrial dysfunction. Functional integrity of mitochondrial DNA from aged subjects. *J. Biol. Chem.* **269**, 6878-6883.

- Holt, I. J., Harding, A. E. and Morgan-Hughes, J. A. (1988). Deletions of muscle mitochondrial DNA in patients with mitochondrial myopathies. *Nature* **331**, 717-719.
- Jishage, M., Fujino, T., Yamazaki, Y., Kuroda, H. and Nakamura, T. (2003). Identification of target genes for EWS/ATF-1 chimeric transcription factor. *Oncogene* **22**, 41-49.
- Kanamori, T., Nishimaki, K., Asoh, S., Ishibashi, Y., Takata, I., Kuwabara, T., Taira, K., Yamaguchi, H., Sugihara, S., Yamazaki, T. et al. (2003). Truncated product of the bifunctional *DLST* gene involved in biogenesis of the respiratory chain. *EMBO J.* **22**, 2913-2923.
- Kang, D. and Hamasaki, N. (2002). Maintenance of mitochondrial DNA integrity: repair and degradation. *Curr. Genet.* **41**, 311-322.
- Kawahara, H., Houdou, S. and Inoue, T. (1991). Scanning electron microscopic observations on muscle cells of experimental mitochondrial myopathy produced by 2, 4-dinitrophenol. *J. Submicrosc. Cytol. Pathol.* **23**, 397-403.
- Klaus, S., Casteilla, L., Bouillaud, F. and Ricquier, D. (1991). The uncoupling protein UCP: a membranous mitochondrial ion carrier exclusively expressed in brown adipose tissue. *Int. J. Biochem.* **23**, 791-801.
- Kobayashi, Y., Momoi, M. Y., Tominaga, K., Momoi, T., Nihei, K., Yanagisawa, M., Kagawa, Y. and Ohta, S. (1990). A point mutation in the mitochondrial tRNA<sup>Leu(UUR)</sup> gene in MELAS (mitochondrial myopathy, encephalopathy, lactic acidosis and stroke-like episodes). *Biochem. Biophys. Res. Commun.* **173**, 816-822.
- Kobayashi, Y., Momoi, M. Y., Tominaga, K., Shimoizumi, H., Nihei, K., Yanagisawa, M., Kagawa, Y. and Ohta, S. (1991). Respiration-deficient cells are caused by a single point mutation in the mitochondrial tRNA<sup>Leu(UUR)</sup> gene in mitochondrial myopathy, encephalopathy, lactic acidosis and stroke-like episodes (MELAS). *Am. J. Hum. Genet.* **49**, 590-599.
- Kowaltowski, A. J. and Vercesi, A. E. (1999). Mitochondrial damage induced by conditions of oxidative stress. *Free Radic. Biol. Med.* **26**, 463-471.
- Kroemer, G. and Reed, J. C. (2000). Mitochondrial control of cell death. *Nat. Med.* **6**, 513-519.
- Liang, P. and Pardee, A. B. (1992). Differential display of eukaryotic messenger RNA by means of the polymerase chain reaction. *Science* **257**, 967-971.
- Lightowlers, R. N., Chinnery, P. F., Turnbull, D. M. and Howell, N. (1997). Mammalian mitochondrial genetics: heredity, heteroplasmy and disease. *Trends Genet.* **13**, 450-455.
- Melov, S. (2000). Mitochondrial oxidative stress. Physiologic consequences and potential for a role in aging. *Ann. New York Acad. Sci.* **908**, 219-225.
- Moraes, C. T., Ricci, E., Bonilla, E., DiMauro, S. and Schon, E. A. (1992). The mitochondrial tRNA<sup>Leu(UUR)</sup> mutation in mitochondrial encephalomyopathy, lactic acidosis and stroke-like episodes (MELAS): genetic, biochemical and morphological correlations in skeletal muscle. *Am. J. Hum. Genet.* **50**, 934-949.
- Moyes, C. D., Mathieu-Costello, O. A., Tsuchiya, N., Filburn, C. and Hansford, R. G. (1997). Mitochondrial biogenesis during cellular differentiation. *Am. J. Physiol.* **272**, C1345-C1351.
- Muller-Hocker, J., Pongratz, D. and Hubner, G. (1986). Activation of mitochondrial ATPase as evidence of loosely coupled oxidative phosphorylation in various skeletal muscle disorders. A histochemical fine-structural study. *J. Neurol. Sci.* **74**, 199-213.
- Munro, S. and Pelham, H. R. (1987). A C-terminal signal prevents secretion of luminal ER proteins. *Cell* **48**, 899-907.
- Nisoli, E., Clementi, E., Paolucci, C., Cozzi, V., Tonello, C., Sciorati, C., Bracale, R., Valerio, A., Francolini, M., Moncada, S. et al. (2003). Mitochondrial biogenesis in mammals: the role of endogenous nitric oxide. *Science* **299**, 896-899.
- Nisoli, E., Falcone, S., Tonello, C., Cozzi, V., Palomba, L., Fiorani, M., Pisconti, A., Brunelli, S., Cardile, A., Francolini, M. et al. (2004). Mitochondrial biogenesis by NO yields functionally active mitochondria in mammals. *Proc. Natl. Acad. Sci. USA* **101**, 16507-16512.
- Ohta, S. (2003). A multi-functional organelle mitochondrion is involved in cell death, proliferation and disease. *Curr. Med. Chem.* **10**, 2485-2494.
- Pfanner, N. and Geissler, A. (2001). Versatility of the mitochondrial protein import machinery. *Nat. Rev. Mol. Cell. Biol.* **2**, 339-349.
- Scarpulla, R. C. (2002). Nuclear activators and coactivators in mammalian mitochondrial biogenesis. *Biochim. Biophys. Acta* **1576**, 1-14.
- Schon, E. A. (2000). Mitochondrial genetics and disease. *Trends Biochem. Sci.* **25**, 555-560.
- Shoubridge, E. A., Karpati, G. and Hastings, K. E. (1990). Deletion mutants are functionally dominant over wild-type mitochondrial genomes in skeletal muscle fiber segments in mitochondrial disease. *Cell* **62**, 43-49.
- Tong, A. H., Lesage, G., Bader, G. D., Ding, H., Xu, H., Xin, X., Young, J., Berriz, G. F., Brost, R. L., Chang, M. et al. (2004). Global mapping of the yeast genetic interaction network. *Science* **303**, 808-813.
- Trounce, I. A., Kim, Y. L., Jun, A. S. and Wallace, D. E. (1996). Assessment of mitochondrial oxidative phosphorylation in patient muscle biopsies, lymphoblasts and transmittochondrial cell lines. *Methods Enzymol.* **264**, 484-509.
- Vorobjev, I. A. and Zorov, D. B. (1983). Diazepam inhibits cell respiration and induces fragmentation of mitochondrial reticulum. *FEBS Lett.* **163**, 311-314.
- Wallace, D. C. (1999). Mitochondrial diseases in man and mouse. *Science* **283**, 1482-1488.
- Weber, K., Ridderskamp, D., Alfert, M., Hoyer, S. and Wiesner, R. J. (2002). Cultivation in glucose-deprived medium stimulates mitochondrial biogenesis and oxidative metabolism in HepG2 hepatoma cells. *Biol. Chem.* **383**, 283-290.
- Wei, Y. F., Robins, P., Carter, K., Caldecott, K., Pappin, D. J., Yu, G. L., Wang, R. P., Shell, B. K., Nash, R. A., Schar, P. et al. (1995). Molecular cloning and expression of human cDNAs encoding a novel DNA ligase IV and DNA ligase III, an enzyme active in DNA repair and recombination. *Mol. Cell. Biol.* **15**, 3206-3216.
- Westermann, B. (2002). Merging mitochondria matters: Cellular role and molecular machinery of mitochondrial fusion. *EMBO Rep.* **3**, 527-531.
- Winzler, E. A., Shoemaker, D. D., Astromoff, A., Liang, H., Anderson, K., Andre, B., Bangham, R., Benito, R., Boeke, J. D., Bussey, H. et al. (1999). Functional characterization of the *S. cerevisiae* genome by gene deletion and parallel analysis. *Science* **285**, 901-906.
- Wu, C. C., Taylor, R. S., Lane, D. R., Ladinsky, M. S., Weisz, J. A. and Howell, K. E. (2000). GMx33: a novel family of trans-Golgi proteins identified by proteomics. *Traffic* **1**, 963-975.
- Yaffe, M. P. (1999). The machinery of mitochondrial inheritance and behavior. *Science* **283**, 1493-1497.
- Zeller, R. (1998). Preparation of cells and tissues for fluorescence microscopy. In *Cells: A Laboratory Manual. Volume 3 Subcellular localization of genes and their products.* (ed. D. L. Spector, R. D. Goldman and L. A. Leinwand), pp. 98.01-98.20. New York: Cold Spring Harbor Laboratory Press.